

AD-A170 936

THE DESIGN OF MODULATION DOPED HETEROSTRUCTURES (II)  
ROYAL SIGNALS AND RADAR ESTABLISHMENT MALVERN (ENGLAND)  
M J KANE ET AL. FEB 86 RSRE-MEMO-3938 DRIC-BR-99917

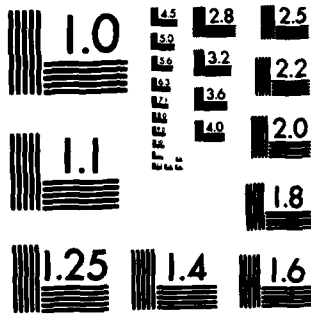
1/1

UNCLASSIFIED

F/C 20/12

NL

END  
DATE  
FILMED  
10-86



MICROCOPY RESOLUTION TEST CHART  
NATIONAL BUREAU OF STANDARDS-1963-A

UNLIMITED

RSRE  
MEMORANDUM No. 3938

**ROYAL SIGNALS & RADAR  
ESTABLISHMENT**

AD-A170 956

THE DESIGN OF MODULATION DOPED HETEROSTRUCTURES

Authors: M J Kane, I W Archibald,  
D A Anderson and P R Tapster

RSRE MEMORANDUM No. 3938

PROCUREMENT EXECUTIVE,  
MINISTRY OF DEFENCE,  
RSRE MALVERN,  
WORCS.

ROYAL SIGNALS AND RADAR ESTABLISHMENT

Memorandum 3938

Title: THE DESIGN OF MODULATION DOPED HETEROSTRUCTURES

Author: M J Kane, I W Archibald, D A Anderson and P R Tapster

Date: February 1986

SUMMARY

This memo presents a set of design rules for the thickness and doping levels of the various layers of a modulation doped heterojunction. It is shown how to optimise the heterostructure so that there is no parasitic parallel conduction and for the maximum low temperature mobility.

Accession For	
NTIS GRA&I	<input checked="" type="checkbox"/>
DTIC TAB	<input type="checkbox"/>
Unannounced	<input type="checkbox"/>
Justification	
By	
Distribution/	
Availability Codes	
Avail and/or	
Dist	Special
A-1	



Copyright  
C  
Controller HMSO London  
1986

RSRE MEMORANDUM NO 3938

THE DESIGN OF MODULATION DOPED HETEROSTRUCTURES

M J Kane, I W Archibald, D A Anderson and P R Tapster

LIST OF CONTENTS

- 1 Introduction
- 2 Potential Profiles
- 3 Mobilities
- 4 Conclusions

Appendix

References

LIST OF FIGURES

- 1a The Structure of a typical modulation doped heterojunction.
- b The electric potential within a modulation doped heterojunction, showing the location of the 2D electron gas.
- 2 The maximum thickness of doped  $\text{Al}_x\text{Ga}_{1-x}\text{As}$  in a modulation doped heterojunction for less than 10% parallel conduction; (ie for the number of carriers in the  $\text{Al}_x\text{Ga}_{1-x}\text{As}$  to be ten times less than the number of carriers in the 2DEG).
- 3a The variation of the 2D electron carrier density with doping level in the  $\text{Al}_x\text{Ga}_{1-x}\text{As}$  for various spacer thicknesses.
- b The data of Figure 3a replotted to show the variation of 2D carrier density with spacer thickness for various doping densities in the  $\text{Al}_x\text{Ga}_{1-x}\text{As}$ .
- 4 The calculated variation of the 2D electron mobility with temperature, showing both the total mobility and the component contributions of various different scattering mechanisms.

## LIST OF FIGURES (Continued)

- 5 The variation of 2D electron mobility at 4.2K with undoped  $\text{Al}_x\text{Ga}_{1-x}\text{As}$  spacer thickness. (The calculation allows for the change in 2D electron density with spacer thickness.) The calculation has been performed for two different values of background impurity density in the GaAs.
- 6a The variation of optimum  $\text{Al}_x\text{Ga}_{1-x}\text{As}$  spacer thickness with  $\text{Al}_x\text{Ga}_{1-x}\text{As}$  doping level for two different values of background impurity levels in the GaAs.
- b The variation of the 2D electron mobility at the optimum spacer thickness of Figure 6a with  $\text{Al}_x\text{Ga}_{1-x}\text{As}$  doping density.

## 1 INTRODUCTION

The technique of modulation doping consists of doping the wider bandgap side of a semiconductor heterojunction. Some of the free electrons created by the doping fall into the narrow bandgap semiconductor where they form a two-dimensional electron gas (2DEG) which is only free to move in the plane of the heterojunction. These free electrons are physically separated from their parent donors so that the reduction in mobility and peak velocity normally associated with increasing the doping do not occur. The three commonest materials systems where this technique is employed are, (with the wide bandgap material mentioned first)  $\text{Al}_x\text{Ga}_{1-x}\text{As}/\text{GaAs}$ ,  $\text{InP}/\text{In}_{0.47}\text{Ga}_{0.53}\text{As}$  and  $\text{Al}_{0.48}\text{In}_{0.52}\text{As}/\text{In}_{0.47}\text{Ga}_{0.53}\text{As}$ . The first mentioned system is grown on GaAs substrates and the latter two on InP.

There exists a large literature on the properties of modulation doped heterojunctions, especially the  $\text{AlGaAs}/\text{GaAs}$  system<sup>(1)-(8)</sup>. Most of the publications consist of short letters and there is as yet a shortage of review

articles on this subject. The purpose of this Memorandum is to present the results of some calculations of the electric potentials, carrier densities, and mobilities in modulation doped heterostructures. The mobility calculations are taken directly from the literature<sup>9,10</sup> but the results are presented in numerical and graphical, rather than algebraic form so that the effects of changing parameters in the heterostructure will be more immediately apparent. Although there is some disagreement between various authors on the absolute values of the mobility limits due to each scattering mechanism the manner in which these vary with parameters such as the 2D electron density, is the subject of much closer agreement. Thus, the absolute values for mobilities quoted later in this paper should be treated with some caution. However, the general trends associated with changing a particular parameter can be regarded as much more reliable.

## 2 POTENTIAL PROFILES

Figure 1a shows the structure of a typical modulation doped heterojunction (MDH). The substrate is semi-insulating GaAs. A layer of GaAs approximately 1  $\mu\text{m}$  thick is grown first. This is followed by an undoped AlGaAs spacer, the doped AlGaAs layer and then a GaAs cap which protects the AlGaAs from atmospheric attack. The spacer layer increases the separation of the free electrons from their parent donors and thereby reduces the remote ionised impurity scattering.

Figure 1b shows the electric potential within an MDH. Some of the electrons from the doped AlGaAs fall into surface traps and create a surface depletion region. Others fall into the 2DEG and create an interface depletion region.

In order to calculate the electric potential within a heterostructure a computer programme capable of simultaneously solving Poisson's equation and equations for the net charge density in a general multilayer system has been written by Dr P Tapster.

Figure 1b is a typical output from this programme.

When designing an MDH the doping and thickness in the AlGaAs and the spacer layer thickness must be chosen so that there is no parasitic conduction in the  $\text{Al}_x\text{Ga}_{1-x}\text{As}$ . (This has deleterious effects on the performance of such structures<sup>11,12</sup>.) Conversely, the thickness of the doped AlGaAs must be the maximum possible for a particular doping level in the  $\text{Al}_x\text{Ga}_{1-x}\text{As}$  if the density of the 2DEG is to be maximised. Figure 2 shows the maximum possible thickness of the AlGaAs for various doping densities.

We have also calculated the variation of the density of the 2DEG ( $N_{2\text{DEG}}$ ) with doping density in the  $\text{Al}_x\text{Ga}_{1-x}\text{As}$  and the spacer layer thickness (with the assumption that the  $\text{Al}_x\text{Ga}_{1-x}\text{As}$  thickness is chosen so that there is no parallel conduction, but only just). Figures 3a and 3b show the calculated values of  $N_{2\text{DEG}}$ . As expected,  $N_{2\text{DEG}}$  increases with increased doping of the AlGaAs and decreases with increased spacer thickness.

It is, however, interesting to note that  $N_{2\text{DEG}}$  is almost independent of  $N_{\text{AlGaAs}}$  when the spacer layer thickness is greater than  $\sim 300 \text{ \AA}$ .

### 3 MOBILITIES

The main reason for employing modulation doped heterostructures is the enhancement in mobility that can be obtained whilst maintaining a high carrier density. This improvement occurs for two reasons:

1. The carriers are separated from their parent donors which eliminates the degradation in electrical properties normally associated with heavy

doping.

ii. The electron gas is degenerate (i.e. the Fermi energy lies in the conduction band).

The scattering mechanisms which determine the mobilities are essentially the same as those which apply in a bulk semiconductor. However, allowance must be made for the two dimensional nature of the conduction band and for the degeneracy. The mechanisms are:

- i. Optical photon scattering.
- ii. Ionised impurity scattering (both remote impurity scattering by donor cores in the AlGaAs and residual impurity scattering by background impurities in the GaAs).
- iii. Acoustic (deformation potential and piezoelectric) phonon scattering.

Figure 4 shows the variation of the total mobility and the component contributions over the temperature range 0-300K. The calculations use results given in references 9 and 10. These should be consulted for details of the calculations. The expressions used for the mobility limits imposed by each scattering mechanism are given in the Appendix.

Optic phonon scattering dominates at room temperature and according to (9) the mobility limit for this mechanism is very close to that found in a bulk semiconductor. The optic phonon energy in GaAs corresponds to a temperature of approximately 410K and the number of these phonons present therefore decreases rapidly as the temperature drops below 300K, giving rise to an increase in the mobility. Other scattering mechanisms, particularly ionised impurity scattering, become significant below  $\sim 100\text{K}$  and optic phonon scattering can be disregarded below  $\sim 60\text{K}$ .

The total cross-section for ionised impurity scattering varies approximately as the inverse square of the energy of the scattered electrons. In a degenerate 2DEG the relevant energy is the Fermi energy, which is only weakly temperature dependent, so that the effects of ionised impurity scattering are almost temperature independent. (In a non-degenerate bulk semiconductor the appropriate energy is the thermal energy  $3/2 kT$ , so that the electron mobility increases with temperature over the range 0 to  $\sim 80K$  where ionised impurity scattering is dominant.)

However, in a degenerate 2DEG the Fermi energy is proportional to the electron density when only one sub-band is occupied. The mobility will therefore increase with carrier density, for a fixed distribution of scatterers.

Deformation potential and piezoelectric phonon scattering become significant below 60K. The decrease in the number of these phonons present is responsible for the increase in the mobility as the temperature decreases below  $\sim 60K$ . When the background impurity density is greater than  $2-3 \times 10^{15} \text{ cm}^{-3}$  in the GaAs the limit on the mobility imposed by residual ionised scattering is much lower than that imposed by acoustic phonon scattering and this mode is almost insignificant.

We have performed self consistent calculations of the mobility of the 2DEG at low temperatures for various structural parameters of the hetero-junction with the aim of optimising the mobility for different values of  $\text{Al}_x\text{Ga}_{1-x}\text{As}$  doping and background impurity levels. (At room temperature optic phonon scattering sets the mobility to a value essentially independent of carrier density.)

The variation of electron mobility with spacer thickness for an  $\text{Al}_x\text{Ga}_{1-x}\text{As}$  doping level of  $10^{18} \text{ cm}^{-3}$  is shown in Figure 5. The initial increase in

mobility with spacer thickness is due to the decrease in the strength of the remote ionised impurity scattering as the donor cores are separated from the electrons. However, increasing the spacer thickness reduces the density of the 2DEG (Figure 3) which tends to reduce the mobility (see above). An increase in mobility with spacer layer thickness will only be obtained when the increased separation of the impurities and the 2DEG more than compensates for the effects of the reduction in the density of the 2DEG, i.e. when remote impurity scattering is more significant than background impurity scattering. When the doping density in the AlGaAs is  $10^{18} \text{ cm}^{-3}$  this crossover occurs at a spacer thickness of 170 Å if the background impurity density is  $10^{15} \text{ cm}^{-3}$  and at 370 Å if the background is  $10^{14} \text{ cm}^{-3}$ . Thick spacers do not result in higher mobilities when the background purity of the GaAs is poor ( $\sim 2 \times 10^{15} \text{ cm}^{-3}$ ). Figure 4 shows that the best mobility possible at 4.2K is  $\sim 3.8 \times 10^5 \text{ cm}^2/\text{Vs}$  with a background impurity level of  $2 \times 10^{15} \text{ cm}^{-3}$ . (These figures only apply to heterojunctions cooled in the dark.) Illumination can introduce extra carriers at the interface without causing additional scattering<sup>5</sup>. We will not consider the effects of illumination in any more detail here.

Figure 6a shows the spacer thickness which gives the maximum mobility for a range of doping densities in the  $\text{Al}_x\text{Ga}_{1-x}\text{As}$ . The optimum spacer thickness is only a weak function of the doping level, provided that this is greater than  $5 \times 10^{17} \text{ cm}^{-3}$ . Figure 6b shows the mobility which will be obtained at the optimum spacer thickness as a function of the AlGaAs doping. Again, provided that the doping is greater than  $5 \times 10^{17} \text{ cm}^{-3}$  only a weak variation is seen.

#### 4 CONCLUSIONS

We have shown that in order to obtain high mobilities in modulation doped heterojunctions high material purity is required ( $< 10^{14} \text{ cm}^{-3}$  impurities in

the GaAs). If this condition is satisfied then a thick spacer will result in a high mobility at low temperatures. If the material purity is low ( $> 10^{15}$   $\text{cm}^{-3}$ ) high mobilities will not be obtained even with thick spacer layers.

## APPENDIX

### THE MATHEMATICAL EXPRESSIONS USED TO CALCULATE THE CONTRIBUTIONS TO THE TOTAL MOBILITY

These expressions are all taken from reference 10.

#### PRELIMINARY DEFINITIONS

- T is the temperature  
k<sub>B</sub> is the Boltzmann constant  
e is the electronic charge  
e<sub>A</sub> is the deformation potential  
ρ is the density  
U<sub>l</sub> is the speed of longitudinal sound waves  
U<sub>t</sub> is the speed of transverse sound waves  
m\* is the effective mass of an electron  
N<sub>2D</sub> is the 2D carrier density  
h<sub>14</sub> is the piezoelectric coupling constant  
ε is the dielectric permittivity  
N<sub>d</sub> is the doping density in the AlGaAs  
d<sub>spacer</sub> is the spacer layer thickness  
N<sub>R</sub> is the background impurity density in the GaAs  
Z<sub>0</sub> is the lateral extent of the 2D wavefunction

$$= \left( \frac{N_{2D}}{10^{12}} \right)^{-1/3} \times 55 \text{ \AA} \quad (N_{2D} \text{ in cm}^{-2})$$

The material parameters used for GaAs in this Memorandum are:

$$\begin{aligned}
 m^* &= 0.067 m_0 \\
 \text{where } m_0 &= 9.11 \times 10^{-31} \\
 \epsilon &= 12.9 \epsilon_0 \\
 \epsilon_0 &= 8.85 \times 10^{-12} \text{ Fm}^{-1} \\
 U_l &= 5.24 \times 10^3 \text{ m s}^{-1} \\
 U_t &= 3.07 \times 10^3 \text{ m s}^{-1} \\
 \rho &= 5.36 \times 10^3 \text{ kg m}^{-3} \\
 e_A &= 11.2 \times 10^{-19} \text{ J} \quad (7 \text{ eV}) \\
 h_{14} &= 1.2 \times 10^5 \text{ V m}^{-1}
 \end{aligned}$$

The mobility limits imposed by the various scattering mechanisms are:

(a) Polar Optic Phonon Scattering

$$\mu_{PO} = \frac{A}{T^2} + \frac{B}{T^6} \quad (\text{A1})$$

$$\begin{aligned}
 \text{where } A &= 7.95 \times 10^8 \text{ cm}^2 \text{ V}^{-1} \text{ s}^{-1} \text{ K}^{-2} \\
 \text{and } B &= 1.18 \times 10^{17} \text{ cm}^2 \text{ V}^{-1} \text{ s}^{-1} \text{ K}^{-6}
 \end{aligned}
 \left. \vphantom{\begin{aligned} \text{where } A \\ \text{and } B \end{aligned}} \right\} \text{ for GaAs}$$

This semi-empirical formula is valid over the temperature range 70-300K where polar optic phonon scattering is significant.

(b) Deformation Potential Scattering

$$\mu_{AC} = \frac{e \hbar^3 \rho b U_l^2}{m^{*2} e_A^2 k_B T} \frac{1}{I_A(\gamma_l)} \quad (\text{A2})$$

$$\text{where } b = 2Z_0$$

$$I_A(\gamma_i) = \left[ \left( \frac{4\gamma_i}{3\pi} \right)^2 + 1 \right]^{\frac{1}{2}}$$

$$\gamma_i = \frac{2\pi U_i q_F}{k_B T}$$

$$q_F = (2\pi N_{2D})^{\frac{1}{2}}$$

and  $U_i = U_l$  or  $U_t$  as appropriate.

(c) Piezoelectric Scattering

$$\mu_{PE} = \frac{32 \hbar^3 \rho \pi q_F}{m^{*2} e k_B T h_{14}^2} \left\{ 9 \frac{I_A(\gamma_l)}{U_l^2} + 13 \frac{I_A(\gamma_t)}{U_t^2} \right\}^{-1} \quad (A3)$$

N.B. Equation (25) of reference 10 contains a printing error. Equation (A3) is derived from a corrected version of this former equation.

(d) Remote Impurity Scattering

$$\mu_{RI} = \frac{64 \pi \hbar^3 \epsilon^2 q_F^3 S_0^2}{e^3 m^{*2}} \frac{1}{(L_1^{-2} - L_2^{-2})} \quad (A4)$$

where  $S_0 = \frac{2e^2 m^*}{4\pi \epsilon h^2}$  - the inverse screening length

$$L_1 = Z_0 + d_{space}$$

and  $L_2 = L_1 + \frac{N_{2D}}{N_d}$

N.B. Equation (12) of reference 10 is incorrect and should be replaced by equation (A4) above. (Equation (26) of reference 10 is correct even though it is nominally derived from the incorrect equation (12).)

(e) Background Impurity Scattering

$$\mu_{BI} = \frac{8\pi n^3 \epsilon^2 q_F^2}{e^3 m^{*2} N_{BI}} \times \frac{1}{I_B(\beta)}$$

where  $\beta = \frac{S_0}{2q_F}$

$$I_B(\beta) = 1.26 \beta^2 + 2.21 \beta + 0.74$$

and  $N_{BI} = N_R Z_0$

The total mobility is given by Matthiessen's rule:

$$\mu^{-1} = \mu_{RI}^{-1} + \mu_{BI}^{-1} + \mu_{PO}^{-1} + \mu_{AC}^{-1} + \mu_{PE}^{-1}$$

## REFERENCES

- 1 H L Stormer, R Dingle, A C Gossard, W Wiegmann and M D Sturge, J Vac Sci Technol 16 1517 (1979).
- 2 H L Stormer, R Dingle, A C Gossard, W Wiegmann and M D Sturge, Solid State Comm 29 705 (1979).
- 3 N Sano, H Kato, S Chika, Solid State Comm 49 123 (1984).
- 4 J C M Hwang, A Kastalsky, H L Stormer and V G Keromidas, Appl Phys Lett 44 802 (1984).
- 5 E E Mendez, P J Price and M Heiblum, Appl Phys Lett 45 294 (1984).
- 6 K Hirakawa, H Sakaki and J Yoshino, Appl Phys Lett 45 253 (1984).
- 7 B F Lin, D C Tsui, M A Paalanen and A C Gossard, Appl Phys Lett 45 695 (1984).
- 8 G Weimann and W Schlapp, Appl Phys Lett 46 411 (1985).
- 9 W Walukiewicz, H E Ruda, J Lagowski and H C Gatos, Phys Rev B30 4571 (1984).
- 10 K Lee, M S Shur, T J Drummond and H Morkoc, J Appl Phys 54 6432 (1983).
- 11 M J Kane, N Apsley, D A Anderson, L L Taylor and T Kerr, J Phys C: Solid State Physics 18 5629 (1985)
- 12 E F Schubert, K Ploog, H Dambkes and K Heime, Appl Phys A33 63 (1984).

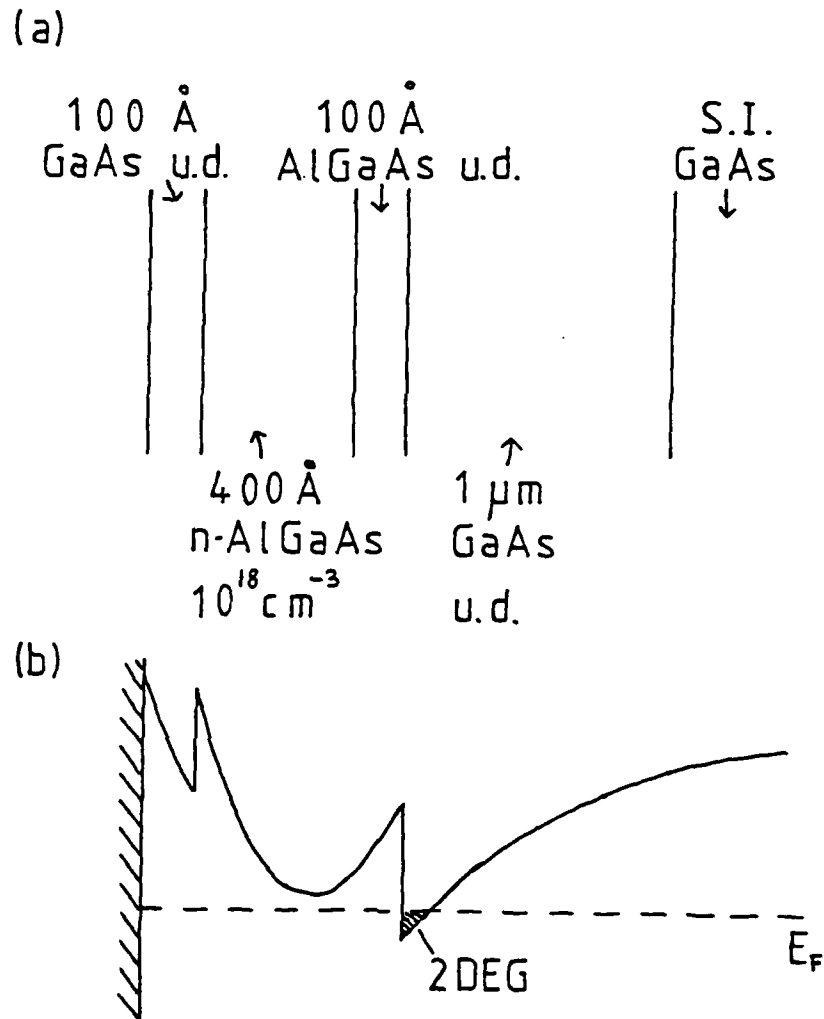


Figure 1

- a The Structure of a typical modulation doped heterojunction.
- b The electric potential within a modulation doped heterojunction, showing the location of the 2D electron gas.

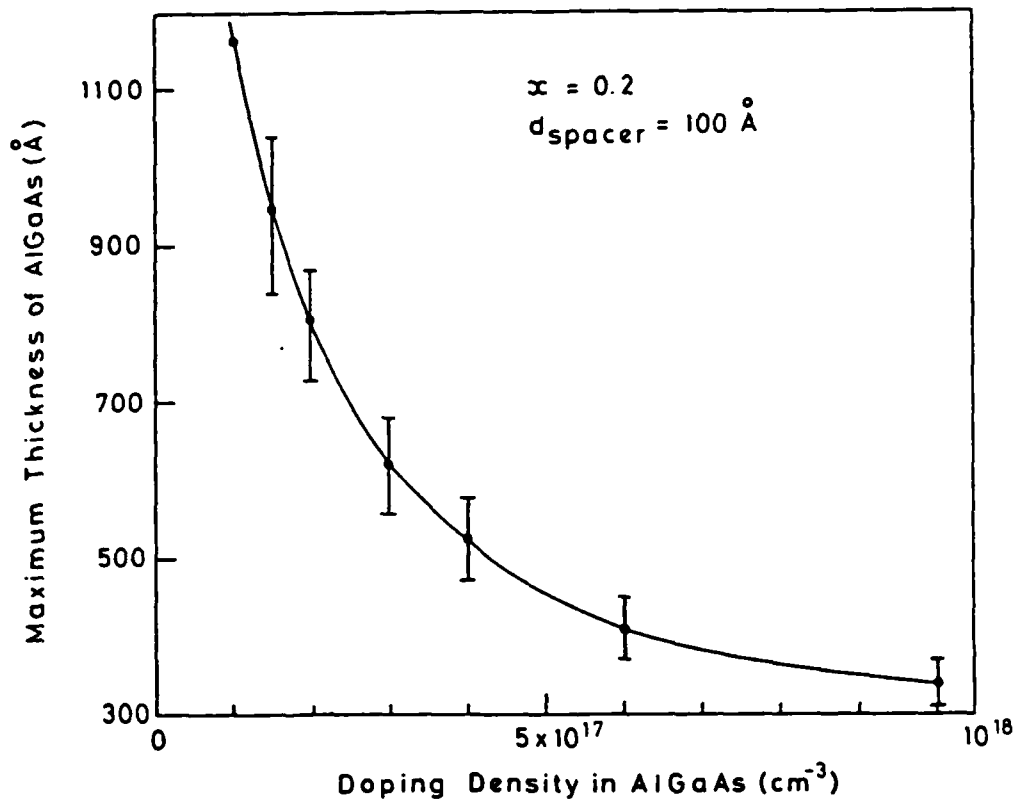


Figure 2

The maximum permissible thickness of  $\text{Al}_x\text{Ga}_{1-x}\text{As}$  in a modulation doped heterojunction for less than 10% parallel conduction, i.e. for the number of carriers in the  $\text{Al}_x\text{Ga}_{1-x}\text{As}$  to be ten times less than the number of carriers in the 2D gas. The error bars represent the permissible variations in the  $\text{Al}_x\text{Ga}_{1-x}\text{As}$  thickness for either a 10% reduction in the density of the 2D electron gas or an additional 10% of parallel conduction. (It is assumed that there are no deep donors in the AlGaAs and quantum size effects are ignored.)

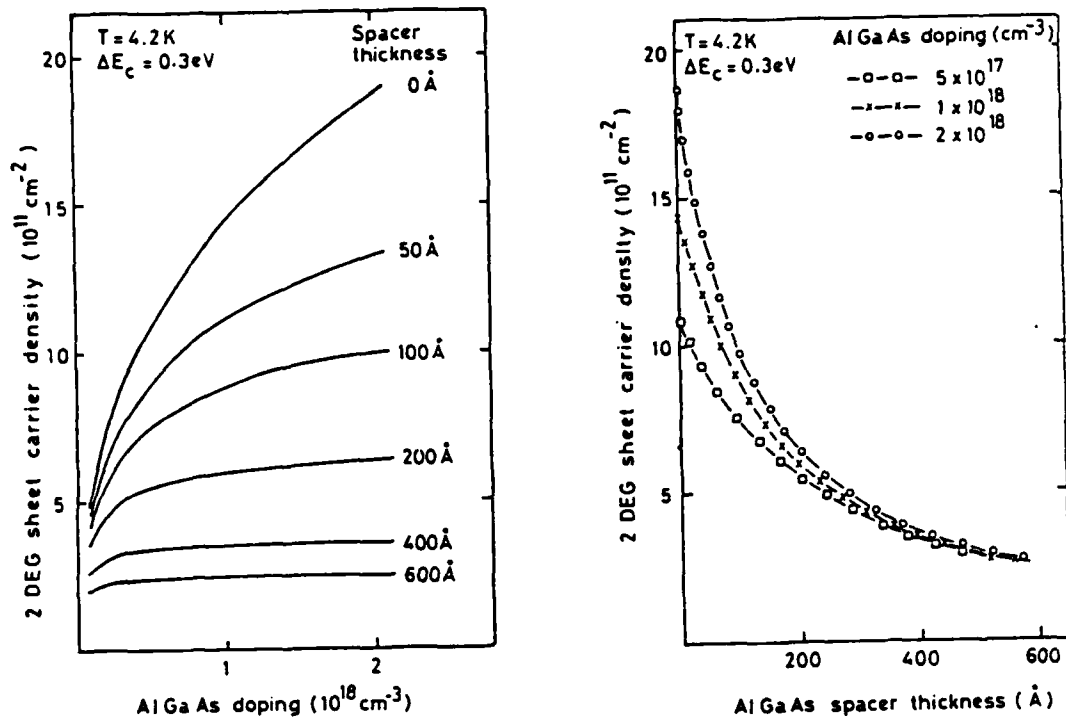


Figure 3

- a The variation of the 2D electron carrier density with doping level in the  $\text{Al}_x\text{Ga}_{1-x}\text{As}$  for various spacer thicknesses.
- b The data of Figure 3a replotted to show the variation of 2D carrier density with spacer thickness for various doping densities in the  $\text{Al}_x\text{Ga}_{1-x}\text{As}$ .

(It is assumed that there are no deep donors in the AlGaAs.)

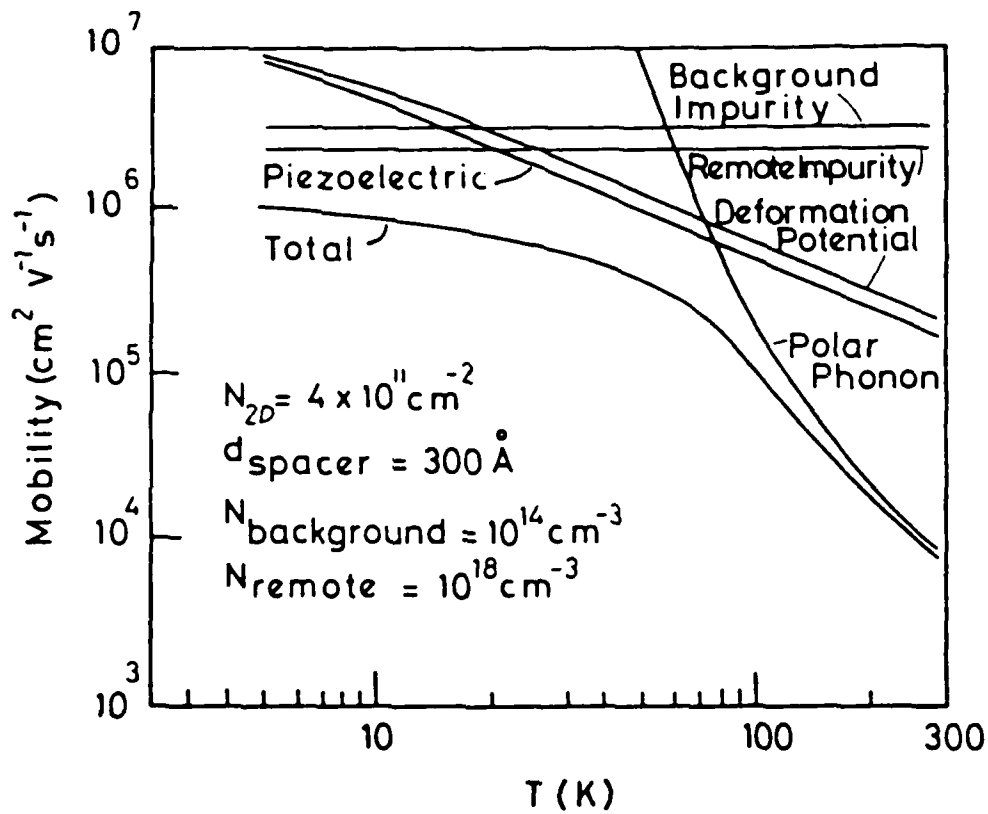
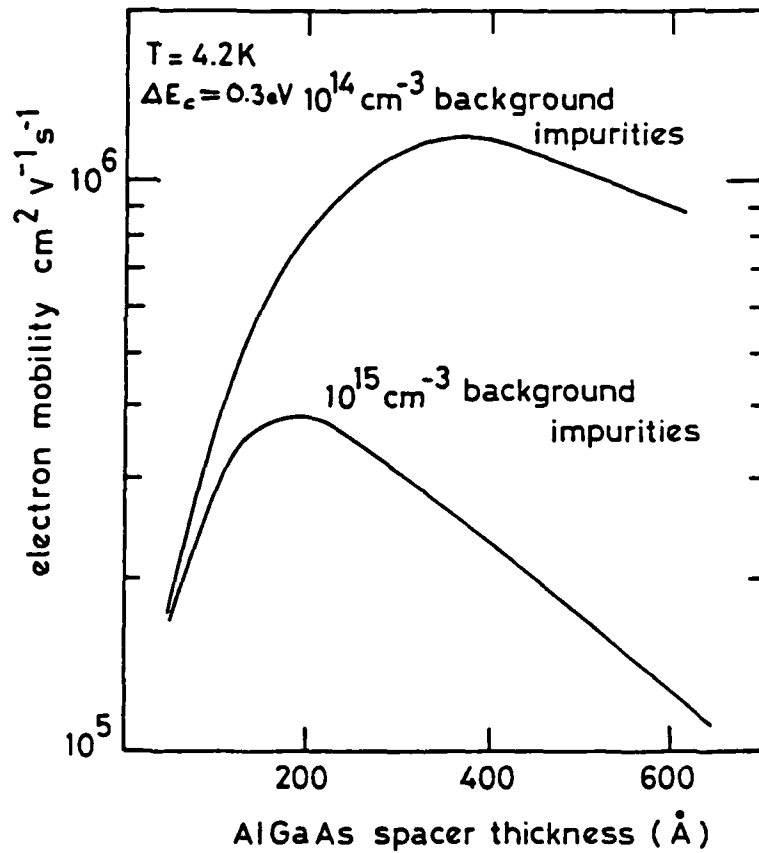


Figure 4

The calculated variation of the 2D electron mobility with temperature, showing both the total mobility and the component contributions of various different scattering mechanisms.



**Figure 5**

The variation of 2D electron mobility at 4.2K with undoped  $\text{Al}_x\text{Ga}_{1-x}\text{As}$  spacer thickness. (The calculation allows for the change in 2D electron density with spacer thickness.) The calculation has been performed for two different values of background impurity density in the GaAs.

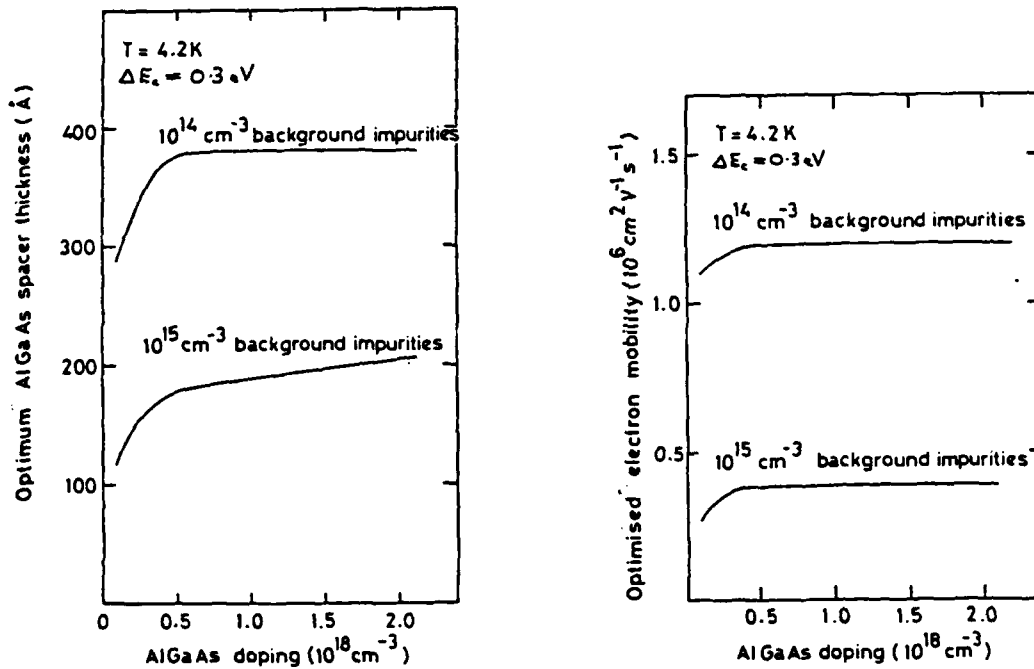


Figure 6

- a The variation of optimum  $\text{Al}_x\text{Ga}_{1-x}\text{As}$  spacer thickness with  $\text{Al}_x\text{Ga}_{1-x}\text{As}$  doping level for two different values of background impurity levels in the GaAs.
- b The variation of the 2D electron mobility at the optimum spacer thickness of Figure 6a with  $\text{Al}_x\text{Ga}_{1-x}\text{As}$  doping density.

DOCUMENT CONTROL SHEET

Overall security classification of sheet ..... UNCLASSIFIED .....

(As far as possible this sheet should contain only unclassified information. If it is necessary to enter classified information, the box concerned must be marked to indicate the classification eg (R) (C) or (S) )

1. DRIC Reference (if known)	2. Originator's Reference Memorandum 3938	3. Agency Reference	4. Report Security U/C Classification	
5. Originator's Code (if known)	6. Originator (Corporate Author) Name and Location Royal Signals and Radar Establishment			
5a. Sponsoring Agency's Code (if known)	6a. Sponsoring Agency (Contract Authority) Name and Location			
7. Title The Design of Modulation Doped Heterostructures				
7a. Title in Foreign Language (in the case of translations)				
7b. Presented at (for conference papers) Title, place and date of conference				
8. Author 1 Surname, Initials Kane M J	9(a) Author 2 Archibald I W	9(b) Authors 3,4... Anderson D A Tapster P R	10. Date	pp. ref.
11. Contract Number	12. Period	13. Project	14. Other Reference	
15. Distribution statement Unlimited				
Descriptors (or keywords)				
continue on separate piece of paper				
<p><b>Abstract</b></p> <p>This memo presents a set of design rules for the thickness and doping levels of the various layers of a modulation doped heterojunction. It is shown how to optimise the heterostructure so that there is no parasitic parallel conduction and for the maximum low temperature mobility.</p>				

DATE  
FILMED  
0-8